JOC The Journal of Organic Chemistry

Note

pubs.acs.org/joc

How Dirhodium Catalyst Controls the Enantioselectivity of [3 + 2]-Cycloaddition between Nitrone and Vinyldiazoacetate: A Density Functional Theory Study

Xin Yang,[‡,†] Yongsheng Yang,[‡] Robert J. Rees,[§] Qi Yang,[†] Zhiyue Tian,[‡] and Ying Xue*[,‡]

[‡]College of Chemistry, Key Lab of Green Chemistry and Technology in Ministry of Education, Sichuan University, Chengdu 610064, P.R. China

[§]Data61 | CSIRO, 343 Royal Parade, Parkville, Victoria 3052, Australia

[†]CSIRO Manufacturing, Bayview Avenue, Clayton, Victoria 3169, Australia

Supporting Information

ABSTRACT: The origin of enantioselectivity in the dirhodium-catalyzed [3 + 2]-cycloaddition of nitrone and vinyldiazoacetate has been investigated using dispersion-corrected density functional theory. Taking a more realistic account of bulky ligands in models of the dirhodium catalyst when investigating its catalytic behavior is crucial for describing the effects resulting from a high level of asymmetric induction. More than one active site can be located and the extra reactivity is provided by an electron-donation interaction between the substrate and an additional Rh_2L_4 catalyst.

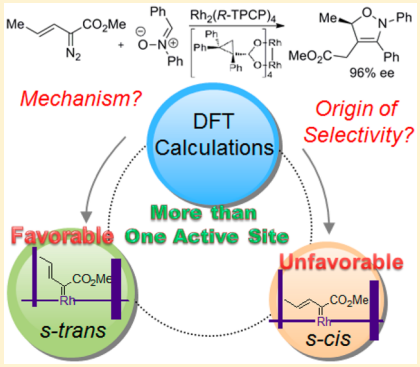

Alkenylcarbene intermediates derived from alkenyldiazo reagents exhibit a high level of regio- or enantioselectivity in [3C + n] cycloadditions (n = 2−4) with small nucleophilic molecules including imines, nitrones, pyrroles, and pyridines to generate various cycloadducts.[1] Among them, dirhodium carbenoids are powerful for asymmetric cycloaddition with nitrones and have been extensively investigated by the groups of Doyle and Davies.[2] These cycloadditions proceed exclusively through an initial generation of dirhodium carbenoids that subsequently react with nitrone nucleophiles to complete cycloadditions, and the reaction selectivity is highly affected by the ligands of the dirhodium catalyst.

The success in the application of dirhodium catalysts results from extensive experimental research into the design of new ligands and the broad spectrum of applications that demonstrates their regio-, chemo-, and enantioselectivities. In addition, quantum chemical calculations have been frequently applied, thus enabling detailed insights into the origin of selectivity in the dirhodium-catalyzed reaction.[3] However, the large size and conformational complexity of the dirhodium catalysts make it challenging to achieve meaningful theoretical treatments using realistic catalyst models even with modern day computing resources. For these reasons, much of the computational work in this field has been carried out using simplified dirhodium catalyst models. For example, the most successful catalyst dirhodium tetracarboxylate Rh_2(S-DOSP)$_4$ is replaced by the $Rh_2(O_2CH)_4$ model (eq 1; Ar = p-($C_{12}H_{25}$)C_6H_4).[4] This widely used procedure has been proven

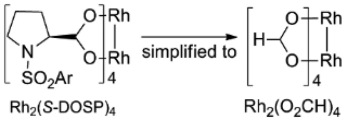

(1)

to be capable of obtaining rational results to explain the experimental results.[4a,b,5] Inspired by the observation that the dirhodium catalyst could have a major effect on the product distribution,[6] we asked the question: can a simplified dirhodium catalyst model qualitatively reflect the subtle steric and electronic effects? Recently, we have investigated the origins of chemoselectivity on catalyst-dependent competitive 1,2-migrations.[7] We found that the popular catalyst model $Rh_2(O_2CH)_4$ fails to explain the high selectivity of three competitive migrations, and the steric and electronic effects of ligands can significantly influence the potential energy surface, which changes the most favorable mechanism and ultimately alters chemoselectivity.

In our efforts exploring the role of dirhodium catalysts, we herein report a comprehensive study of the reaction mechanism of Rh_2(R-TPCP)$_4$-catalyzed enantioselective [3 + 2]-cycloaddition between vinyldiazoacetate **1** and nitrone **2** as shown in eq 2.[2b] To do this, we performed density functional theory (DFT) calculations (for more details, see part I in the Supporting Information). The computations demonstrate the

Received: June 21, 2016
Published: July 27, 2016

DOI: 10.1021/acs.joc.6b01447
J. Org. Chem. 2016, 81, 8082−8086

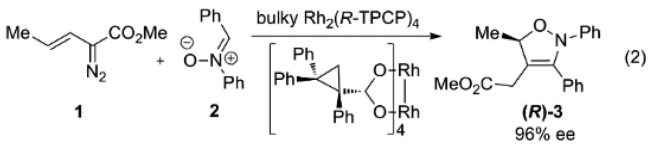

important role of bulky ligands and explore how the dirhodium catalyst controls, in particular, the enantioselectivity in an unexpected way. Significantly, it is shown that chiral bulky dirhodium catalyst can enhance reactivity through more than one active site.

First, we examined the possible mechanism proposed by Davies et al. (Figure 1).[2b] The overall reaction occurs through a two-step sequential annulation (**I**)/catalyst dissociation (**II**) pathway. In step I, Rh_2L_4-carbenoid **4** activates the adjacent vinyl group for vinylogous nucleophilic attack by nitrone **2**, followed by [3 + 2]-cyclization to form five-membered ring intermediate **B**. In step **II**, **B** either undergoes 1,3-hydrogen migration followed by a proton transfer (donated as step **II**-type A) or goes through 1,2-hydrogen migration followed alkene isomerization (donated as step **II**-type B) to form the product (***R***)-**3**.

Here, we emphasize three key points: (1) our mechanistic studies focus on the catalytic cycle starting from the Rh_2L_4-carbenes because previous DFT calculations have already exposed the detailed processes of Rh_2L_4-carbene formation from α-diazocarbonyl compounds;[3b,4b,5e] (2) on the basis of the stereochemical model proposed by the Davies and Musaev groups,[8] this type of dirhodium catalyst preferentially exists in a D_2 symmetric conformation, and the chiral influence can be represented by steric blocking groups as indicated in Figure 2a, allowing for reaction to occur at the Rh_2L_4-carbene *Si*-face, which is therefore the only attack side we took into consideration; and (3) similar to Davies' results,[4a] we found that there is no strongly preferred conformer of the *s-cis* or *s-trans* conformations, which readily interconvert (Table S1). Thus, neither of them can be ruled out at this stage, and they should be considered for subsequent reactions even though the [3 + 2]-cycloadduct (***S***)-**3** derived from the *s-cis* conformer is not observed experimentally. With two possible orientations of nitrone, this leads to four possible approach combinations as illustrated in Figure 2b. The combinations can be considered to be endolike or exolike in analogy to the relative location

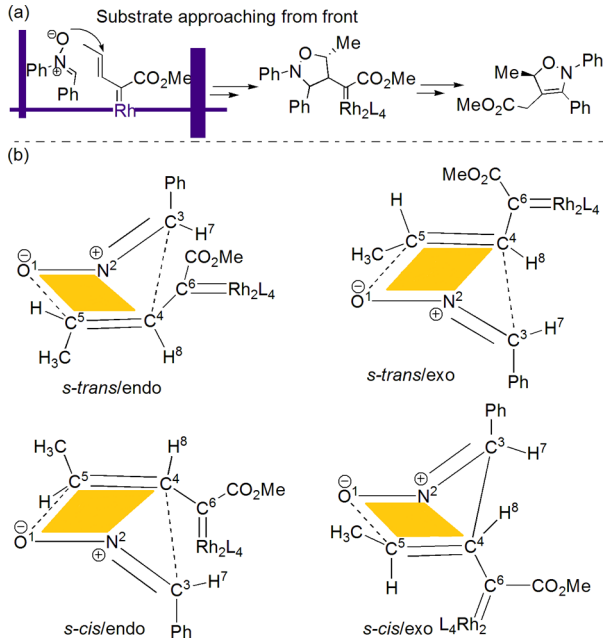

Figure 2. (a) Predictive model for asymmetric induction. (b) Combinations of nitrone approaches and vinylcarbene conformations.

between bulky group on C^4 and the Ph group connected to C^3 on corresponding five-membered ring **B** and are therefore classified based on this in addition to the conformation of the vinylcarbenoid (*s-trans*/endo, etc.). In the following section, we will describe a detailed evaluation of reactions through all four possible combinations. To represent the mechanisms in a simpler way, we name all of the possible intermediates and transition states using the prefixes **td**, **tx**, **cd**, and **cx** to represent those involved in *s-**t**rans*/en**d**o, *s-**t**rans*/e**x**o, *s-**c**is*/en**d**o, *s-**c**is*/e**x**o combinations, respectively.

Using the Simplified $Rh_2(O_2CH)_4$ Model. The calculations show that the nucleophilic attack of nitrone **2** to **4** via step **I** is very facile (Figure 3). First, we investigated step **II**-type A for the subsequent catalyst dissociation (Figure 3, Figure S4). It was found that the 1,3-hydrogen migration (**TS-III**) in exocombination is significantly favored over that in endocombination. This is because in (**tx**)-**B** and (**cx**)-**B**, the H^7 atom (the migrating hydrogen atom) is *cis* to the carbene carbon C^6,

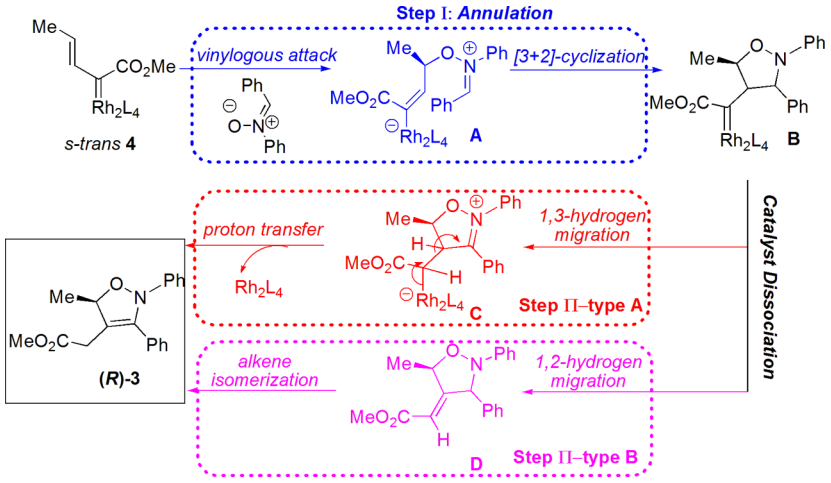

Figure 1. Possible mechanism proposed by Davies group.[2b]

DOI: 10.1021/acs.joc.6b01447
J. Org. Chem. 2016, 81, 8082−8086

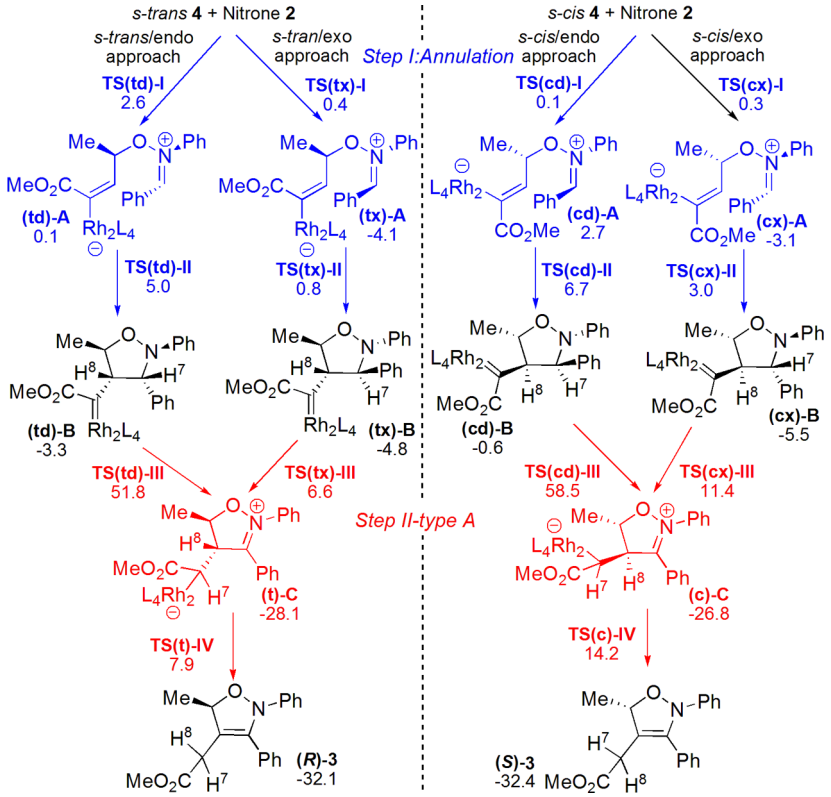

Figure 3. Calculated pathway (via step **I** (blue) and step **II**-type A (red)) for $Rh_2(O_2CH)_4$-catalyzed [3 + 2]-cycloaddition of vinylcarbenoid **4** and nitrones **2**. Energies (kcal mol^{-1}) are relative to *s-trans* vinycarbenoid **4** and nitrone **2** and calculated using (SMD)M06-GD3/BS2//M06-GD3/BS1.

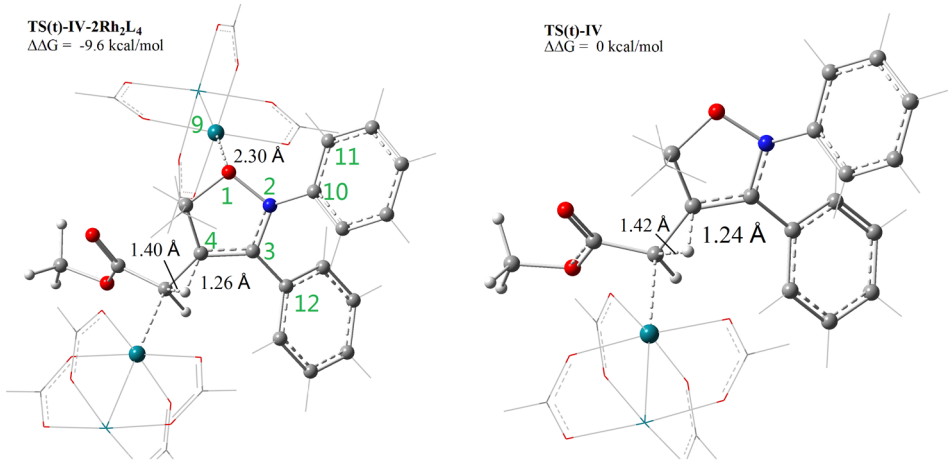

Donor (i)	Acceptor (j)	E(2)[a] (kcal/mol)	E(j)-E(i)[b] (a.u.)	F(i,j)[c] (a.u.)
LP(1) O^1	LP* Rh^9	10.25	1.61	0.117
LP(2) O^1	LP* Rh^9	21.21	1.57	0.165

[a] E(2) means energy of hyperconjugative interactions
[b] energy difference between donor and acceptor i and j NBO orbitals
[c] F(i,j) is the Fock matrix element between i and j NBO orbitals

Figure 4. Optimized transition structures **TS(t)-IV-2Rh$_2$L$_4$** and **TS(t)-IV** and the second order perturbation theory analysis of the Fock matrix in NBO basis for **TS(t)-IV-2Rh$_2$L$_4$**. Energies are calculated using (SMD)M06-GD3/BS2//M06-GD3/BS1. Some parts of molecules are illustrated in wireframe for clarity.

whereas it is *trans* to the carbene group in **(td)-B** and **(cd)-B** (Figures S5 and S6). The H^7 orientation toward the carbene carbon atom is crucial because it brings about significant C−H/π interaction on **TS(tx)-III** and **TS(cx)-III**. Furthermore, in **TS(tx)-III** and **TS(cx)-III**, the bulky Rh_2L_4 group and the phenyl group on C^3 point in opposite directions, thereby reducing steric repulsion. In contrast, **TS(td)-III** and **TS(cd)-III** lack the C−H/π interaction and suffer from steric crowding between the phenyl group and the bulky Rh_2L_4 group. This significant decrease in the energy barrier for 1,3-hydrogen migration **TS-III** (43.7 and 42.3 kcal mol^{-1} energy barrier decrease from **TS(td)-III** to **TS(tx)-III** and from **TS(cd)-III** to

DOI: 10.1021/acs.joc.6b01447
J. Org. Chem. 2016, 81, 8082−8086

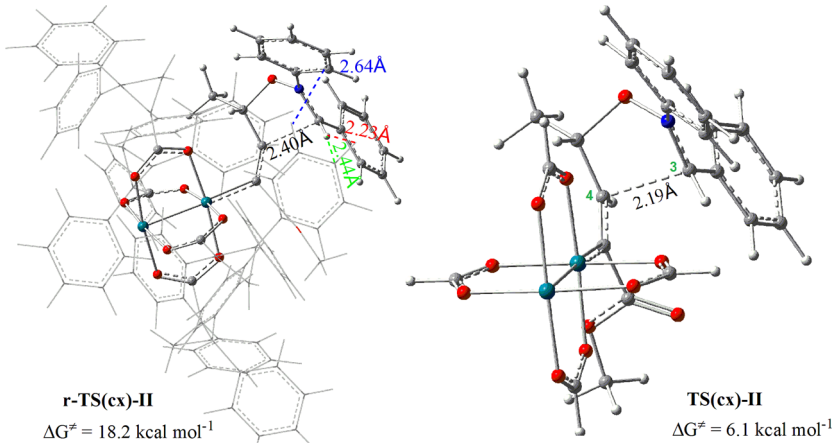

Figure 5. Transition structures **r-TS(cx)-II** and **TS(cx)-II** for the Rh_2L_4-catalyzed [3 + 2]-cycloaddition between vinylcarbenoid and nitrone. Energies were calculated at the (SMD)M06-GD3/BS2//M06-GD3/BS1 level of theory and are reported relative to *s-cis* vinylcarbenoid **r-4** + nitrone **2** and *s-cis* **4** + **2**, respectively. The bulky ligands on Rh_2(*R*-TPCP)$_4$ are illustrated in wireframe for clarity.

TS(cx)-III, respectively) leads to the exciting possibility that, even though the step **II**-type A mechanism was found to be kinetically unfeasible, other possible mechanisms may be accessible by using the appropriate combination of dirhodium carbenoid and nitrone (this has been confirmed by our later calculations).

Next to be considered is step **II**-type B, which includes 1,2-hydrogen migration followed by alkene isomerization (for more details, see page S12 in the Supporting Information and Figures S7−S11). The calculations show that the 1,2-hydrogen migration via **TS-V** starting from five-membered ring **B** is very facile, and the subsequent stepwise or concerted alkene isomerization suffers at least a 37.9 kcal mol^{-1} free energy barrier (from **(td)-B** via **(td)-E-(c)** to the product **(*R*)-3**; Figure S7). Therefore, the catalyst dissociation via the step **II**-type B pathway is kinetically unfeasible in light of the fact that the dirhodium-catalyzed [3 + 2]-cycloaddition can smoothly occur at room temperature.

Reviewing all of the aforementioned energy surfaces (Figures S4 and S11), we conclude that starting from four possible combinations, step **I** (annulation) is energetically favored but step **II** (catalyst dissociation) suffers a very high free energy barrier. Many attempts to achieve a reasonable free energy barrier were unfortunately unsuccessful. However, an unexpected energy barrier decline for proton transfer was observed when additional Rh_2L_4 was associated with O^1 atom on five-membered ring intermediate **B**. The computed activation free energies for proton transfer via transition state **TS(t)-IV-2Rh$_2$L$_4$** and **TS(c)-IV-2Rh$_2$L$_4$** are 9.6 and 13.3 kcal mol^{-1} lower than those via **TS(t)-IV** and **TS(c)-IV**, respectively (Figure 4, Figure S12). This is a surprising result because dirhodium-catalyzed [3C + *n*]-cycloaddition is typically considered as only one dirhodium molecule-catalyzed reaction. The natural bond orbital (NBO) analysis[9] clearly shows the donation from the lone pair (LP) of the O^1 atom to the associated Rh[9] LP* orbital in **TS(t)-IV-2Rh$_2$L$_4$** and **TS(c)-IV-2Rh$_2$L$_4$**, which can result in stabilization of the transition states. In addition, the orbital overlap at the five-membered ring and the conjugated phenyl rings clearly demonstrate strong delocalization. The electron cloud movement from donor to acceptor can make the molecule highly polarized. Therefore, proton transfer should be beneficial from such delocalization. The facility of protonation with additional Rh_2L_4 is also well-reflected by a more advanced transition state (lengths of the breaking C^4−H^8 bonds are 1.26 vs 1.24 and 1.26 vs 1.25 Å, and those of forming C^6−H^8 bonds are 1.40 vs 1.42 and 1.39 vs 1.40 Å in **TS(t)-IV-2Rh$_2$L$_4$** vs **TS(t)-IV** and **TS(c)-IV-2Rh$_2$L$_4$** vs **TS(c)-IV**, respectively). As can be seen, the additional Rh_2L_4 intrinsically acts as an activator for the partial activation of C^4−H^8. Therefore, coupled with the results that the 1,3-hydrogen migration in s-*trans*/endo and s-*cis*/endo approach combinations suffers from great steric repulsion effects between bulky Rh_2L_4 (the one connected to C^6) and the phenyl group connected to C^3 (Figures S5 and S6), we concluded that, with the aid of two dirhodium catalyst molecules, the substrate (nitrone) attacks vinylcarbenoid in a s-*trans*/exo or s-*cis*/exo approach combination to form **(*R*)-3** or **(*S*)-3**, respectively. The formation of **(*R*)-3** and **(*S*)-3** with additional Rh_2L_4 has an overall activation free energy of 24.5 and 24.3 kcal mol^{-1}, respectively. These nearly the same overall free energy barriers suggest that the [3 + 2]-cycloadditions from *s-cis* and *s-trans* conformers are competitive with each other. Consequently, the **(*S*)-3** product derived from *s-cis* vinylcarbene can certainly not be ruled out solely on the basis of the free energy barriers using simplified catalyst model $Rh_2(O_2CH)_4$, which is inconsistent with the high enantioselectivity observed experimentally.

We expected that the bulky ligands on Rh_2L_4 would be required to enhance the enantioselectivity. Therefore, we decided to explore the effect of bulky ligands on the reaction of nitrone and vinylcarbene **r-4** by replacing the simplified catalyst model $Rh_2(O_2CH)_4$ by the realistic chiral catalyst Rh_2(*R*-TPCP)$_4$ (below, we use the prefix **r-** to describe all the transition states and intermediates involved in realistic Rh_2(*R*-TPCP)$_4$-catalyzed reaction mechanisms).

Using the Realistic Dirhodium Catalyst. Thermodynamically, *s-cis* **r-4** and *s-trans* **r-4** have similar energy (Figure S13), which is the same as that using simplified model $Rh_2(O_2CH)_4$ (for the calculation details, see page S21 in the Supporting Information) . A remarkable difference between pathways involving *s-trans* and *s-cis* conformers is that the annulation (step **I**) for the *s-trans* conformer is still facile, similar to the case when using simplified model $Rh_2(O_2CH)_4$, whereas it becomes much more unfavorable for the *s-cis* conformer, which is apparently a consequence of the steric interference of substrate nitrone with the bulky ligands on dirhodium catalyst in *s-cis* conformation (Figure 5). The

DOI: 10.1021/acs.joc.6b01447
J. Org. Chem. 2016, 81, 8082−8086

stronger steric interaction of bulky ligands on dirhodium catalyst with nitrone is also well-reflected by its significantly longer C^3-C^4 bond length (C^3-C^4 = 2.40 Å in **r-TS(cx)-II** vs 2.28 Å in **r-TS(tx)-II**, Figure S14). DFT calculations show that the [3 + 2]-cyclization from *s-trans* **r-4** to give **r-(tx)-B** has an overall activation free energy of 9.6 kcal mol^{-1}, which is 8.6 kcal mol^{-1} lower than that from *s-cis* **r-4** (Figure 6). The big difference in energy, therefore, indicates that the *s-trans* conformer is much more favored when the bulky chair dirhodium complex is used as the catalyst.

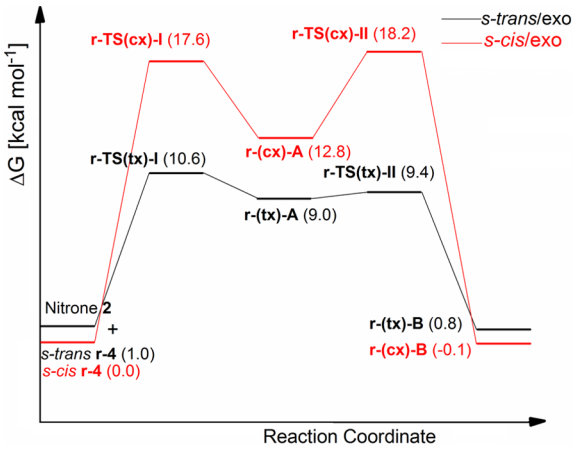

Figure 6. Gibbs free energy profile of the Rh_2(*R*-TPCP)$_4$-catalyzed [3 + 2]-cycloaddition between vinylcarbenoid and nitrone. Energies (kcal mol^{-1}) are relative to *s-cis* vinycarbenoid **r-4** and nitrone **2** and calculated using (SMD)M06-GD3/BS2//M06-GD3/BS1.

Several important conclusions can be gained from these computations: *s-cis* vinylcarbenoid **1** as well as *s-trans* vinylcarbenoid **1** clearly represent likely reactants in the [3 + 2]-cycloaddition reaction. However, bulky-Rh_2L_4-catalyzed annulation of vinyldiazoacetate affords a preferred *s-trans* dirhodium carbenoid to minimize the steric repulsion between the substrate nitrone and the "wall" of Rh_2L_4. This steric effect of the bulky ligands plays a crucial role in the stereochemical outcome. Although a simplified model system is important for the study of elementary reaction steps, care must be taken when results are extrapolated to a more realistic case, especially when steric effect would play a key role in the catalytic systems. Moreover, it is found for the first time that, in dirhodium-catalyzed cycloaddition reactions, additional Rh_2L_4 is unexpectedly essential to facilitate the proton transfer. These findings may have broad implications in understanding and developing dirhodium-catalyzed reactions.

■ ASSOCIATED CONTENT

Supporting Information

The Supporting Information is available free of charge on the ACS Publications website at DOI: 10.1021/acs.joc.6b01447.

Computational details and additional calculated results (PDF)

■ AUTHOR INFORMATION

Corresponding Author

*E-mail: yxue@scu.edu.cn.

Notes

The authors declare no competing financial interest.

■ ACKNOWLEDGMENTS

This project has been supported by the National Natural Science Foundation of China (Grant Nos. 21573153 and 21173151).

■ REFERENCES

(1) (a) Davies, H. M. L.; Beckwith, R. E. J. *Chem. Rev.* **2003**, *103*, 2861−2904. (b) Shapiro, N. D.; Toste, F. D. *Synlett* **2010**, *5*, 675. (c) Barluenga, J.; Lonzi, G.; Riesgo, L.; López, L. A.; Tomás, M. *J. Am. Chem. Soc.* **2010**, *132*, 13200−13202. (d) Reddy, R. P.; Davies, H. M. L. *J. Am. Chem. Soc.* **2007**, *129*, 10312−10313. (e) Deng, L.; Giessert, A. J.; Gerlitz, O. O.; Dai, X.; Diver, S. T.; Davies, H. M. L. *J. Am. Chem. Soc.* **2005**, *127*, 1342−1343. (f) Davies, H. M. L.; Xiang, B.; Kong, N.; Stafford, D. G. *J. Am. Chem. Soc.* **2001**, *123*, 7461−7462. (g) Liu, Y.; Bakshi, K.; Zavalij, P.; Doyle, M. P. *Org. Lett.* **2010**, *12*, 4304−4307.

(2) (a) Wang, X.; Xu, X.; Zavalij, P. Y.; Doyle, M. P. *J. Am. Chem. Soc.* **2011**, *133*, 16402−16405. (b) Qin, C.; Davies, H. M. L. *J. Am. Chem. Soc.* **2013**, *135*, 14516−14519. (c) Wang, X.; Abrahams, Q. M.; Zavalij, P. Y.; Doyle, M. P. *Angew. Chem., Int. Ed.* **2012**, *51*, 5907−5910. (d) Wang, X.; Abrahams, Q. M.; Zavalij, P. Y.; Doyle, M. P. *Angew. Chem.* **2012**, *124*, 6009−6012.

(3) (a) Liang, Y.; Zhou, H.; Yu, Z.-X. *J. Am. Chem. Soc.* **2009**, *131*, 17783−17785. (b) Nakamura, E.; Yoshikai, N.; Yamanaka, M. *J. Am. Chem. Soc.* **2002**, *124*, 7181−7192.

(4) (a) Hansen, J. H.; Gregg, T. M.; Ovalles, S. R.; Lian, Y.; Autschbach, J.; Davies, H. M. L. *J. Am. Chem. Soc.* **2011**, *133*, 5076−5085. (b) Nowlan, D. T.; Gregg, T. M.; Davies, H. M. L.; Singleton, D. A. *J. Am. Chem. Soc.* **2003**, *125*, 15902−15911. (c) Li, Z.; Boyarskikh, V.; Hansen, J. H.; Autschbach, J.; Musaev, D. G.; Davies, H. M. L. *J. Am. Chem. Soc.* **2012**, *134*, 15497−15504.

(5) (a) Bonge, H. T.; Hansen, T. *Tetrahedron Lett.* **2010**, *51*, 5298−5301. (b) Briones, J. F.; Hansen, J.; Hardcastle, K. I.; Autschbach, J.; Davies, H. M. L. *J. Am. Chem. Soc.* **2010**, *132*, 17211−17215. (c) Li, Z.; Boyarskikh, V.; Hansen, J. H.; Autschbach, J.; Musaev, D. G.; Davies, H. M. L. *J. Am. Chem. Soc.* **2012**, *134*, 15497−15504. (d) Zhang, X.; Ke, Z.; DeYonker, N. J.; Xu, H.; Li, Z.-F.; Xu, X.; Zhang, X.; Su, C.-Y.; Phillips, D. L.; Zhao, C. *J. Org. Chem.* **2013**, *78*, 12460−12468. (e) Hansen, J.; Autschbach, J.; Davies, H. M. L. *J. Org. Chem.* **2009**, *74*, 6555−6563. (f) Hansen, J. r.; Li, B.; Dikarev, E.; Autschbach, J.; Davies, H. M. L. *J. Org. Chem.* **2009**, *74*, 6564−6571. (g) Bonge, H. T.; Hansen, T. *J. Org. Chem.* **2010**, *75*, 2309−2320. (h) DeAngelis, A.; Shurtleff, V. W.; Dmitrenko, O.; Fox, J. M. *J. Am. Chem. Soc.* **2011**, *133*, 1650−1653. (i) Xie, Q.; Song, X.-S.; Qu, D.; Guo, L.-P.; Xie, Z.-Z. *Organometallics* **2015**, *34*, 3112−3119.

(6) Davies, H. M. L.; Stafford, D. G.; Hansen, T. *Org. Lett.* **1999**, *1*, 233−236.

(7) Yang, X.; Yang, Y.; Xue, Y. *ACS Catal.* **2016**, *6*, 162−175.

(8) Qin, C.; Boyarskikh, V.; Hansen, J. H.; Hardcastle, K. I.; Musaev, D. G.; Davies, H. M. L. *J. Am. Chem. Soc.* **2011**, *133*, 19198−19204.

(9) Glendening, E.; Reed, A.; Carpenter, J.; Weinhold, F. *NBO*, version 3.1, TCI. University of Wisconsin: Madison, WI, 1998; *65*.

DOI: 10.1021/acs.joc.6b01447
J. Org. Chem. 2016, 81, 8082−8086